Theoretical Studies Concerning the Optimization of Conjugated Molecules for Third-Order Nonlinear Optics

Eric E. Moore and David Yaron*

Department of Chemistry, Carnegie Mellon University, Pittsburgh, Pennsylvania 15213

Received: August 2, 2001; In Final Form: March 13, 2002

Within Hückel theory, the nonresonant third-order nonlinear optical susceptibility of a conjugated polymer is directly proportional to the bandwidth raised to the third power, and inversely proportional to the optical gap raised to the sixth power. This functional dependence, if correct, implies that polyacetylene is already an optimal organic material with regards to the magnitude of the nonresonant hyperpolarizability. Therefore, any improvements in the figure-of-merit for optical switching applications will come at the expense of the magnitude of the hyperpolarizability. Here, singles configuration-interaction (S-CI) theory is used to solve the Pariser−Parr−Pople (PPP) Hamiltonian of polyacetylene, treating both the strength of electron−electron interactions and the degree of bond alternation as model parameters. The results show that the hyperpolarizability is independent of the strength of electron−electron interactions and thus the degree of electron−hole correlation, and instead depends almost exclusively on the optical gap and the bandwidth. Furthermore, the functional dependence on the optical gap and bandwidth is nearly identical to that obtained from Hückel theory, giving strong support to the Hückel description of long chains, and its implications for materials optimization. In addition, the inverse-sixth power dependence of the hyperpolarizability is shown to imply a strong dependence of the transition moments on the optical gap. Finally, the resonant hyperpolarizability associated with two-photon absorption is found to tend toward an inverse-sixth power dependence on optical gap, although deviations from this dependence are considerably larger than for the resonant response.

I. Introduction

This paper explores the factors that establish the magnitude of the third-order nonlinear optical susceptibility of conjugated organic systems. We begin by considering the nonresonant third-order nonlinear optical response,[1,2] using polyacetylene as a reference system. Although the nonresonant response of polyacetylene is among the largest of any known material,[3] the properties of this material still fall short of those needed for optical switching applications.[4] We also consider two photon absorption, a resonant third-order nonlinear optical process with applications in biological imaging and optical fabrication.[5−7] In particular, we consider whether the conclusions obtained for the nonresonant response apply also to this resonant response.

In considering the optimization of the nonresonant hyperpolarizability, a central issue is whether Hückel theory captures the essentials of the nonlinear optical response. This issue is central because Hückel theory implies that, at least with regards to the magnitude of the nonresonant response, polyacetylene is already an optimal organic material. Within Hückel theory, polyacetylene is a one-dimensional semiconductor with two π-electron bands, one valence band and one conduction band.[8,9] The properties of these bands are set by the transfer integrals for the single and double bonds, β_1 and β_2. The bond alternation, $2|\beta_1 - \beta_2|$, sets the band gap, while $2|\beta_1 + \beta_2|$ sets the distance between the bottom of the valence band and the top of the conduction band, thereby establishing the bandwidth. The third-order nonlinear optical susceptibility, γ, can be obtained analytically, and the result scales approximately as[9]

$$\gamma \propto \sigma \frac{|\beta_1+\beta_2|^3}{E_g^{\,6}} \qquad (1)$$

where σ is the density of π-electrons, and E_g is the gap, $E_g = 2|\beta_1 - \beta_2|$. Equation 1 indicates that the response is directly proportional to the density of π-electrons and the bandwidth, and inversely proportional to the band gap. Hückel theory then suggests three ways to increase the magnitude of the nonresonant response. The first is to increase $|\beta_1 + \beta_2|$ and thus the total bandwidth of the system. However, increasing $|\beta_1 + \beta_2|$ is not easily accomplished because the overall magnitude of β is a fundamental property of the carbon−carbon multiple bond and is not amenable to synthetic control. The second way to increase the response is to lower the band gap. Although this can be accomplished synthetically by lowering the effective bond alternation, $|\beta_1 - \beta_2|$, the band gap of polyacetylene is already quite low. If the gap were lowered further, it is likely that the benefits resulting from an increase in the magnitude of the nonresonant hyperpolarizability would be more than offset by increased optical loss at the frequencies of relevance to device design.[4] Finally, the response can be improved by increasing the density of π-electrons but, since all of the non-hydrogen atoms are involved in the π network, this is also nearly optimal in polyacetylene.

The above argument implies that polyacetylene is optimal with regards to the magnitude of the nonresonant hyperpolarizability, but not necessarily with regards to the figure of merit for optical switching applications.[4] However, optimizing other aspects of the figure of merit will likely come at the expense of lowering the magnitude of the nonresonant response. For instance, an important parameter in the figure of merit for optical switching applications is the optical loss of the material. As alluded to above, this places a lower limit on the optical gap of the material. In addition, the absorption spectrum of polyacetylene exhibits a low-energy absorption tail that increases the

10.1021/jp012999y CCC: $22.00
Published on Web 04/30/2002

optical loss and thus lowers the figure of merit. Alternative structures, such as those that introduce phenyl rings into the main chain, may eliminate the low-energy absorption tail and lower the optical loss. However, phenyl rings increase the effective bond alternation[10] and thus decrease the per-chain hyperpolarizability. They also introduce higher-energy pi-bands, such that not all of the pi-electron density participates in the lowest energy excitation where it can contribute optimally to the nonresonant response.

So within Hückel theory, it is not clear how to design a conjugated polymer that significantly improves on polyacetylene. However, the reliability of Hückel theory remains an open issue. For instance, it is well-known that Hückel theory fails to correctly describe, even qualitatively, many aspects of the two-photon excited states that mediate the nonlinear optical response.[10−14] For short polyenes, detailed comparisons between the nonlinear optical response predicted by Hückel theory and that obtained from exact solutions of Pariser−Parr−Pople (PPP) theory show substantial differences,[15,16] even when the parameters are adjusted such that both theories give the same optical gap. In addition, using an anharmonic oscillator model on the PPP Hamiltonian, Mukamel and co-workers[17,18] concluded that electron−hole correlation plays a central role in establishing the nonresonant response.

Despite the above indications that Hückel theory is not sufficient to describe the hyperpolarizability, there is some evidence that its predictions are valid in the limit of long chains. For instance, the predictions of Hückel theory for the nonresonant response of long polymer chains are in reasonable agreement with experiment.[19−22] A rationale for the reliability of Hückel theory in the long-chain limit is that it captures the essentials of the mechanism that dominates the response of long chains. In Hückel theory, the large nonlinear optical response results from two-photon processes in which the first photon promotes an electron from a valence to a conduction band, thereby creating an electron−hole pair, and the second photon operates on the electron or hole created by the first photon.[23,24] Such two-photon processes are very nonlinear because, in effect, the first photon sees an insulator while the second photon sees a conductor. Although conjugated molecules possess many electronic states that are not of this single electron−hole pair character, it is plausable that (i) the nonresonant response is dominated by single electron−hole pair states, and that (ii) Hückel theory captures the essentials of the two-photon processes mediated by these single electron−hole pair states. (Note that because the Hückel parameters are adjusted to give the bandwidth and optical gap obtained either experimentally or from higher-level theories, it is the functional dependence on bandwidth and optical gap of eq 1 that is being tested, not the ability of Hückel theory to predict the bandwidth or optical gap.)

In ref 24, we tested the first of the above two conjectures by comparing a single electron−hole pair theory with a higher-level theory, using the PPP model of polyacetylene as a test system. The single electron−hole pair theory was singles configuration interaction (S-CI) theory, which describes the excited states as linear combinations of all possible single electron−hole pair configurations. The higher-level theory was a scattering formalism that includes double electron−hole configurations in a manner that allows for size-consistent calculations on long polymer chains. The inclusion of double electron−hole pair configurations introduces new classes of states, such as low-lying A_g symmetry states and states containing two excitons. Despite the introduction of these new classes of states, the nonresonant third-order hyperpolarizability agrees with that from S-CI theory. This agreement indicates that these new classes of states have little impact on the nonresonant response of a long chain, and that single electron−hole pair states dominate the response. A more detailed discussion of the validity of S-CI theory is given below in section 2.1.

Our goal here is to test the second of the above two conjectures by comparing the predictions of Hückel theory with those of S-CI theory for a broad range of model parameters. The validity of the functional relation in eq 1 is of particular interest because this relation underpins the above arguments regarding materials optimization. In Hückel theory, the electrons and holes do not interact with one another, and all states contain free electron−hole pairs. It is not surprising, therefore, that the hyperpolarizability depends only on the band gap for creation of electron−hole pairs, and the bandwidth that characterizes their motion. In S-CI theory, the Coulomb interactions between the electron and hole cause their motion to become correlated. Coulomb interactions can, for instance, lead to the formation of bound electron−hole pairs or excitons. It seems reasonable to expect that the hyperpolarizability will depend on the strength of these Coulomb interactions, such that the simple functional dependence of eq 1 holds only in the limit of vanishing electron−hole interactions. However, in ref 23, we showed that, for the PPP model of polyacetylene with standard Ohno parametrization,[25] the nonresonant hyperpolarizability of S-CI theory agrees with that obtained from Hückel theory, provided that the Hückel parameters are adjusted to yield the same optical gap as S-CI theory. This suggests that the nonresonant hyperpolarizability is insensitive to electron−hole interactions, but the comparison was done for only one set of parameters and so may not be general.

Here, we examine the nonresonant hyperpolarizability predicted by S-CI theory for a broad range of model parameters, and show that the functional dependence on the optical gap and bandwidth is nearly identical to that of eq 1, predicted by Hückel theory. The results therefore support the conclusions arrived at above regarding materials optimization.

This paper also briefly considers the resonant response associated with two-photon absorption, to see whether optimization of this resonant response is fundamentally different than optimization of the nonresonant response. Brédas, Marder, and co-workers[26−28] have suggested a chromophore design strategy based on acceptor−donor−acceptor (A−D−A) and donor−acceptor−donor (D−A−D) symmetric charge-transfer systems. The A−D−A systems consist of linear conjugated molecules with electron acceptors on both ends and electron donors in the center. This pattern is reversed in D−A−D systems. Here, we use an internal field to model the effects of the acceptors and donors. Once again, the magnitude of the resonant response shows a dependence on optical gap that is similar to Hückel theory, although the variance is larger than that observed for the nonresonant response.

II. Computational Methods

A. Nonresonant Calculations. The nonresonant calculations are done on a periodic polyacetylene structure, with carbon−carbon double and single bond lengths of 1.35 and 1.46 Å, and bond angles of 120°. We treat PPP theory as a 3 parameter model. Two of these parameters are the transfer integrals $\alpha_{ij} = \beta_1$ (β_2) for single (double) bonds, and one parameter, S_{e-e}, sets the strength of electron−electron interactions. The Hamiltonian

is then[11]

$$H_{\mathrm{PPP}} = \sum_{i,j,\sigma} [-I\delta_{i,j} + \alpha_{j,i}]\, a^{\dagger}_{j,\sigma}\, a_{i,\sigma} + \frac{1}{2}\sum_{i} U(\hat{\rho}_i - 1)\hat{\rho}_i + \sum_{i<j} U(r_{j,i})\hat{\rho}_j\hat{\rho}_i \qquad (2)$$

where $a^{\dagger}_{i,\sigma}(a_{i,\sigma})$ creates (destroys) an electron with spin σ in the p-orbital on the i^{th} carbon, $\hat{\rho}_i$ is the charge operator on the i^{th} carbon, $\hat{\rho}_i = 1 - a^{\dagger}_{i,\alpha}a_{i,\alpha} - a^{\dagger}_{i,\beta}a_{i,\beta}$, and $r_{i,j}$ is the distance between carbons i and j. Both the electron−electron repulsion and the electron−nuclear attraction are described with the following scaled Ohno potential[29]

$$U(r) = S_{e-e}\frac{14.397\mathrm{eV\AA}}{\sqrt{(14.397\mathrm{eV\AA}/U)^2 + r^2}} \qquad (3)$$

where U is the Hubbard parameter. The parameter S_{e-e} sets the strength of electron−electron interactions, and is equal to one for the PPP model,[11] and zero for Hückel theory. I and U are chosen such that application of the Hamiltonian to a single carbon atom yields the ionization potential and electron affinity of an sp^2 hybridized carbon, $I = 11.16$ eV and $U = 11.13$ eV.[30]

In Hückel theory, the transfer integrals establish both the band gap and bandwidth. The band gap is set by the difference between the transfer integrals, $2|\beta_1 - \beta_2|$. The difference in energy between the top of the conduction band and the bottom of the valence band (the total bandwidth) is $2|\beta_1 + \beta_2|$. In the Hückel model, all of the excited states contain free electron−hole pairs and the band gap, for creation of free charges, is equal to the optical gap, the energy of the lowest allowed optical state. In the PPP model, electron−electron interactions may lead to the formation of bound electron hole pairs or excitons. Because the exciton carries optical intensity and lies lower in energy than the free electron−hole pair states, the optical gap is lower than the band gap. In PPP theory, the optical and band gaps depend on the transfer integrals, β_1 and β_2 and the strength of electron−electron interactions, S_{e-e}. PPP calculations on polyenes typically use $\beta_1 = -2.228$ eV and $\beta_2 = -2.581$ eV. Unless otherwise stated, in this paper we fix the sum of the transfer integrals $|\beta_1 + \beta_2|$ at 5.0 eV, and treat $|\beta_1 - \beta_2|$ as an adjustable parameter. We then explore the dependence of the hyperpolarizability on two parameters, S_{e-e} and the difference between the transfer integrals $|\beta_1 - \beta_2|$.

To connect the nonlinear optical response to the structure of the excited electronic states, we work within the sum-over-states formalism for the nonresonant hyperpolarizability[1]

$$\gamma_{xxxx} = \gamma_{+} - \gamma_{-} \qquad (4)$$

$$\gamma_{+} = \sum_{A,B,C}\frac{\langle GS|\hat{x}|A\rangle\langle A|\hat{x}|B\rangle\langle B|\hat{x}|C\rangle\langle C|\hat{x}|GS\rangle}{E_{\mathrm{A}}E_{\mathrm{B}}E_{\mathrm{C}}} \qquad (5)$$

$$\gamma_{-} = \sum_{A,C}\frac{\langle GS|\hat{x}|A\rangle\langle A|\hat{x}|GS\rangle\langle GS|\hat{x}|C\rangle\langle C|\hat{x}|GS\rangle}{E_{\mathrm{A}}{}^{2}E_{\mathrm{C}}} \qquad (6)$$

where $|GS\rangle$ is the ground electronic state, $|A\rangle$, $|B\rangle$, and $|C\rangle$ are excited electronic states, E_I is the energy of state $|I\rangle$ relative to the ground state, and $\langle I|\hat{x}|J\rangle$ are the matrix elements of the transition moment along the x axis, which is chosen to lie parallel to the polymer backbone.

The nonresonant calculations presented below are done on a polyacetylene chain with N_{cell} double bonds and periodic boundary conditions.[23,24] Unless otherwise noted, all calculations are done with $N_{\mathrm{cell}} = 81$. A transition moment operator, $\hat{x}$ of eq 5, that is consistent with periodic boundary conditions is obtained by using the $\hat{x}$ operator appropriate for a ring of $2N_{\mathrm{cell}}$ carbon atoms.[23,24,31] In the long chain limit, γ_{xxxx} of a ring is $^3/_8{}^{\mathrm{th}}$ that of a linear chain with the same number of unit cells.[23,24] We remove this geometric factor by multiplying γ_{xxxx} of the ring by $^8/_3$. The γ_{xxxx}'s reported here thus reflect those of a long, linear chain. Note that the ring geometry is used only to obtain a periodic transition moment operator. The Hamiltonian parameters used are those appropriate for a linear chain because inclusion of curvature effects in the Hamiltonian would serve only to slow convergence to the long-chain limit.

The excited states used in eq 5 are generated using S-CI theory and a complete basis of all singly excited configurations. In periodic boundary conditions, the one-dimensional crystal momentum, k, is a good quantum number. The selection rule for optical transitions is $\Delta k = \pm\, ^{2\pi}/_{L}$, where L is the length of the polymer, or equivalently the circumference of the ring used for the $\hat{x}$ operator. The one-photon allowed states will therefore have $k = ^{2\pi}/_{L}$ and ^1B_u symmetry. The energy of the lowest such state is identified as the optical gap. The two-photon allowed states will have either $k = 0$ or $k = ^{4\pi}/_{L}$. The m^1A_g state is defined as the two-photon state that has the largest transition moment with the 1^1B_u state. In S-CI calculations with periodic boundary conditions, this is the lowest state with ^1A_g symmetry, and so here, the m^1A_g state is assigned to the lowest allowed two-photon state. The band, or free-charge, gap is assigned to the energy of the Hartree−Fock HOMO−LUMO gap, since it is at this energy that unbound electron−hole pair states appear in a S-CI calculation.

The S-CI calculations performed here constrain the excited states to contain one electron and one hole. This approximation requires some justification, as it is well established that double excitations must be included to obtain even a qualitatively valid description of some of the electronic states of polyenes, most notably the 2^1A_g state.[10,11] Despite the large effects that doubly excited configurations can have on specific excited states, there is the following strong evidence that S-CI theory provides a valid description of the nonresonant response.

First, Mazumdar and co-workers[12−14] examined exact solutions of the PPP model for polyenes with up to 12 carbon atoms using a wide range of Hamiltonian parameters. Based on these calculations, they identified three excited states that dominate the nonlinear optical response, the 1^1B_u, m^1A_g, and n^1B_u states. The 1^1B_u state carries most of the one-photon intensity. The m^1A_g state lies above the 1^1B_u state and carries most of the two-photon intensity. The n^1B_u state is a high energy state that has a large transition moment with the m^1A_g state. Abe and co-workers[32−34] identified a similar set of essential states when using singles-configuration interaction (S-CI) theory to model third harmonic generation spectra. Within S-CI theory, the 1^1B_u and m^1A_g states contain a bound electron−hole pair and the n^1B_u state is a nearly free electron−hole pair state that occurs at the edge of the conduction band. Mazumdar and co-workers have given similar qualitative interpretations to the essential states of their model. That S-CI theory and exact solutions of the PPP model agree on the nature of the 1^1B_u, m^1A_g, and n^1B_u states suggests that S-CI theory provides a valid description of the dominant pathways establishing the nonresonant hyperpolarizability.

Another indication that doubly excited configurations are not important in nonresonant calculations comes from considering

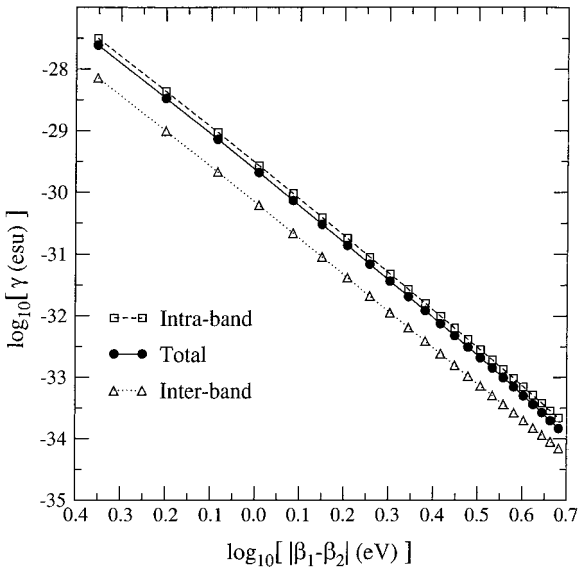

Figure 1. Log−log plot of the hyperpolarizability obtained from Hückel calculations on polyacetylene, as a function of $|\beta_1 - \beta_2|$ for $(\beta_1 + \beta_2) = -5$ eV. The breakdown into inter-band and intra-band contributions is described in section 2.1.

the approximations involved in applying S-CI theory to the Hückel Hamiltonian. Because the $\hat{x}$ operator is a one-electron operator, the one photon states, A and C in eqs 5 and 6, must contain a single electron−hole pair. The two-photon states, B in γ_+ of eq 5, may contain either one or two electron−hole pairs. Because S-CI theory restricts B to states containing a single electron−hole pair, the summation in γ_+ is over two-photon processes in which the first photon creates an electron−hole pair and the second photon moves either the electron or the hole within the one-dimensional band structure. This is the intra-band term,[9,23,24] and it dominates the hyperpolarizability. The approximation involved in S-CI theory is the omission of those terms in γ_+ in which B contains two electron−hole pairs.[37] These terms correspond to two-photon processes in which both the first and second photon create an electron−hole pair. If the two electron−hole pairs do not interact, then their contribution to γ_+ is identically canceled by terms appearing in γ_-. This cancellation makes sense because the creation of two noninteracting excitations does not correspond to a nonlinear process and so should not contribute to the hyperpolarizability. In Hückel theory, the electron−hole pairs interact only through Pauli-exclusion, whereby the electron−hole pair created by the first photon suppresses formation of an additional electron−hole pair. This "saturable absorbance" or "inter-band" contribution[9,24] leads to a small decrease in the hyperpolarizability. So within Hückel theory, the approximations involved in S-CI theory are equivalent to neglecting the negative inter-band or saturable absorbance contribution to the hyperpolarizability. However, the unique aspect of conjugated polymers is the large positive hyperpolarizability, which arises from the intra-band contribution and dominates the nonlinear response (this it illustrated further in Figure 1 of section 3.1).

When applied to the Hückel Hamiltonian, S-CI theory captures the intra-band contribution that dominates the hyperpolarizability of conjugated polymers. In the PPP Hamiltonian, electron−electron interactions lead to a number of new effects. One such effect is the correlation between the motion of the electron and hole in the single electron−hole pair states, and this effect is captured by S-CI theory. But electron−electron interactions introduce other effects that are not captured by S-CI theory and that could potentially alter the hyperpolarizability. Consider, for instance, a two-photon process in which two electron−hole pairs are created. In a model that includes electron−electron interactions, these electron−hole pairs may interact through Coulomb forces in addition to the Pauli exclusion interactions present in Hückel theory. Also, electron−electron interactions may lead to a strong mixing between single and double electron−hole pair configurations and the consequent formation of low-energy ^1A_g symmetry states.[10,11] In a previous work,[24] we developed a scattering formalism that includes both of these effects. Those results indicate that, although inclusion of double electron−hole pair configurations has a large effect on the structure of the excited states, the nonresonant hyperpolarizability of a long chain is nearly identical to that obtained from S-CI theory. This strongly suggests that S-CI theory provides a valid description of the nonresonant hyperpolarizability.

B. Resonant Calculations. The A−D−A and D−A−D systems of Brédas, Marder, and co-workers[26−28] are modeled by applying an internal field to a polyene with 20 carbon atoms. The internal field is zero at the center of the polyene and either increases (D−A−D) or decreases (A−D−A) linearly with distance from the center. The Hamiltonian is then

$$H_{\mathrm{PPP}} + \sum_i V|x_i|\hat{\rho}_i \tag{7}$$

where H_{PPP} is given in eq 2, V is a free parameter describing the strength of the acceptors and donors, and x_i is the x-coordinate of the i^{th} atom relative to the molecular center.

The nonlinear hyperpolarizability $\gamma(-\omega_s; \omega_1, \omega_2, \omega_3)$ is calculated using eq 6.37 of ref 35. The m^1A_g state is identified as the state with the largest transition moment to the 1^1B_u state. The 2-photon absorption cross section to the m^1A_g state is calculated as $\mathrm{Im}\gamma(-\omega; \omega, -\omega, \omega)$, with ω equal to half the energy of the m^1A_g state.

III. Results

A. Nonresonant Hyperpolarizability. We begin by examining the magnitude of the intra-band and inter-band contributions of Hückel theory. Section 2 pointed out that S-CI theory does not include double electron−hole pair states. It therefore includes the intra-band contribution to the hyperpolarizability, but ignores the inter-band (saturable absorbance) contribution.[9,23,24] The relative importance of these terms within Hückel theory is examined in Figure 1, which shows both the intra-band and inter-band contributions as a function of $|\beta_1 - \beta_2|$, with $(\beta_1 + \beta_2)$ fixed at -5 eV. The results indicate that the intra-band term dominates the hyperpolarizability over a wide range of band gap. The ratio of the inter-band to intra-band term remains relatively fixed, changing from 22% to 33% as the band gap, $2|\beta_1 - \beta_2|$, increases from 0.9 to 9.6 eV. The weak dependence of this ratio on band gap may be rationalized as follows. As $|\beta_1 - \beta_2|$ approaches $|\beta_1 + \beta_2|$, β_1 approaches zero and the system approaches a collection of noninteracting ethylene units. In this limit, the system is no longer a semiconductor and the inter-band, saturable absorbance, contribution begins to dominate. But even with $|\beta_1 - \beta_2| = 4.8$ eV and $|\beta_1 + \beta_2| = 5$ eV, for which the band gap is 9.6 eV and the bands are only 0.2 eV wide, the system is sufficiently semiconducting that the hyperpolarizability is dominated by the intra-band contribution.

In Figures 2-4, we examine the dependence of various calculated quantities on S_{e-e} of eq 3, which sets the strength of electron−electron interactions.

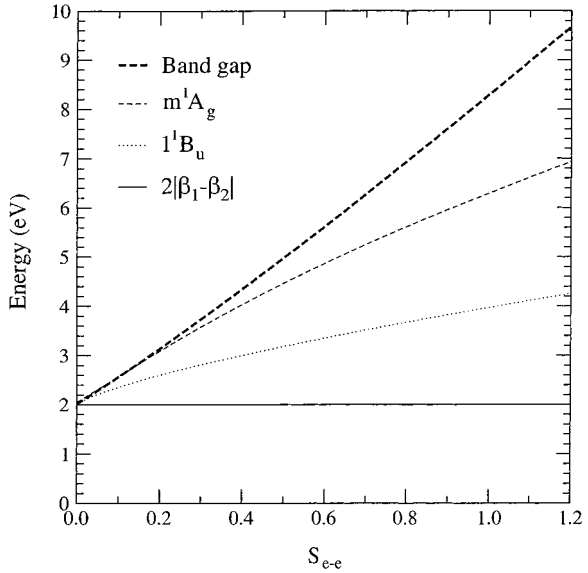

Figure 2. State energies as a function of the strength of electron−electron interactions, S_{e-e} in eq 3. The one-electron-transfer integrals are fixed at $\beta_1 = -2.0$ eV and $\beta_2 = -3.0$ eV, corresponding to a Hückel gap, $2|\beta_1 - \beta_2|$, of 2.0 eV. The band gap is the Hartree−Fock HOMO−LUMO gap, at which free electron−hole pairs states appear in S-CI theory. All results are for S-CI calculations on a chain with 81 unit cells, using periodic boundary conditions.

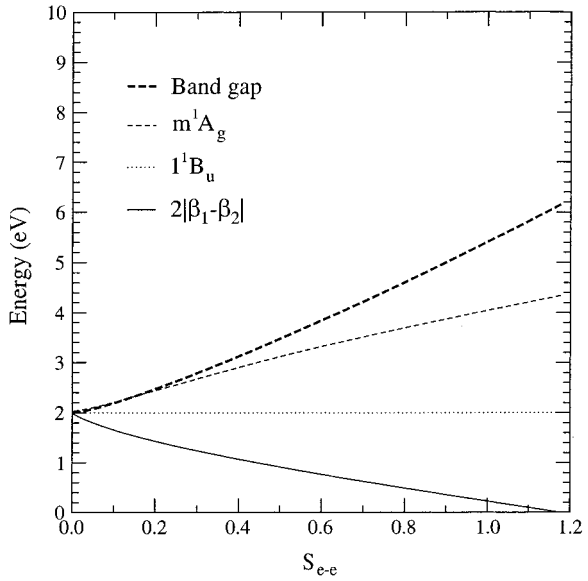

Figure 3. State energies as a function of the strength of electron−electron interactions, S_{e-e} in eq 3, holding the optical gap fixed. The calculations are similar to those in Figure 2, except the bond alternation $|\beta_1 - \beta_2|$ is adjusted to maintain a constant optical gap of 2.0 eV.

Figure 2 shows the energy of the essential states as a function of S_{e-e}. The bond alternation, $|\beta_1 - \beta_2|$, is fixed at 1.0 eV, corresponding to a Hückel gap of 2.0 eV. As S_{e-e} is increased, the difference between the optical gap 1^1B_u state and the band (free-charge) gap is increased. This is an indication of exciton formation, with the difference being the exciton binding energy. The binding energy of the m^1A_g state, a higher-lying exciton state that carries most of the two-photon intensity, also increases with S_{e-e}. An important feature of these results is that, in addition to raising the exciton binding energies, increasing S_{e-e} causes an increase in both the optical gap and the energy of the m^1A_g state.

Figure 4 demonstrates that increasing the strength of electron−electron interactions, in the manner of Figure 2, leads to a

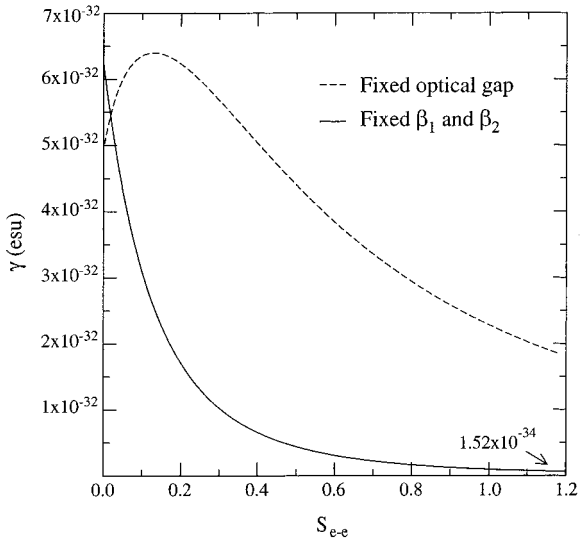

Figure 4. Calculated hyperpolarizabilities for the systems of Figures 2 and 3.

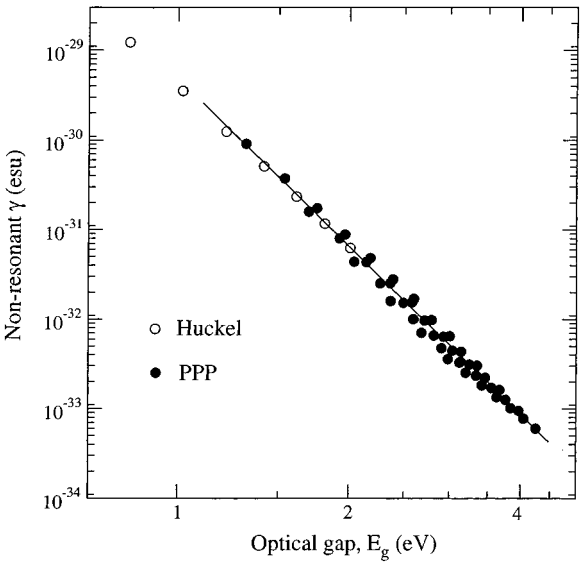

Figure 5. Log−log plot of the nonresonant hyperpolarizability versus the optical gap obtained from S-CI calculations on a polyacetylene chain with 81 unit cells, using both the Hückel and PPP Hamiltonian. In both the Hückel and PPP calculations, $\beta_1 + \beta_2 = -5.0$, and results are shown for $|\beta_1 - \beta_2| = 0.4$ through 1.0 eV in increments of 0.1 eV. The Hückel results (S_{e-e}=0.0) are shown as open circles, and the PPP results ($S_{e-e} = 0.2$ to 1.2 in increments of 0.2) are shown as filled circles. To be consistent with S-CI theory, the Hückel calculations contain only the migration contribution to the hyperpolarizability (see section 2). The solid line is a least-squares fit to the PPP data, showing $\gamma \propto E_g^{-6.1}$.

substantial lowering of the hyperpolarizability. This strong effect of electron−electron interactions seems to argue against the use of Hückel theory to model the nonresonant nonlinear optical response of conjugated polymers.[17,18] However, in Hückel calculations, the parameters are typically adjusted to reproduce the optical gap of the material. A better comparison is then to examine the dependence on the strength of electron−electron interactions while holding the optical gap fixed. This is shown in Figure 3, where S_{e-e} is varied over the same range as in Figure 2 but where the bond alternation, $|\beta_1 - \beta_2|$, is adjusted to maintain a constant optical gap. Just as in Figure 2, increasing S_{e-e} leads to an increase in the exciton binding energies and the energy of the m^1A_g state. However, Figure 4 shows that the

calculated hyperpolarizability varies by only about a factor of 3, as opposed to the nearly 2 orders of magnitude observed when S_{e-e} was increased without holding the optical gap fixed. This indicates that the hyperpolarizability is primarily a function of the optical gap and not the exciton binding energy, as we will now examine in more detail.

Figure 5 provides a more detailed comparison between S-CI calculations performed on the PPP and Hückel Hamiltonians. According to the Hückel relation of eq 1, the nonresonant hyperpolarizability scales as $\gamma \propto E_g^{-6}$. The open circles of Figure 5 show results obtained from Hückel theory, holding the sum of the transfer integrals fixed at $(\beta_1 + \beta_2) = -5.0$ eV, and varying $|\beta_1 - \beta_2|$ between 0.4 and 1.0 eV. On this log−log plot, the Hückel results fall on a line with slope −6, as expected because $\gamma \propto E_g^{-6}$. The closed circles of Figure 5 show the results of PPP calculations obtained by varying $|\beta_1 - \beta_2|$ between 0.4 and 1.0 eV and S_{e-e} from 0.2 to 1.0. The PPP results are nearly collinear, with a slope of −6.1. This indicates that $\gamma \propto E_g^{-6.1}$, which is nearly identical to the behavior of Hückel theory in eq 1.

The dependence of the nonresonant hyperpolaribility on the optical gap, $\gamma \propto E_g^{-6}$, has consequences for the transition moments between the essential excited states. In the essential-states model,[12−14] the 1^1B_u state carries most of the intensity out of the ground electronic state and the m^1A_g state carries most of the intensity out of the 1^1B_u state. The hyperpolarizability of eq 5 may then be written

$$\gamma = \frac{|\langle GS|\hat{x}|1^1B_u\rangle|^2 |\langle 1^1B_u|\hat{x}|m^1A_g\rangle|^2}{E_g{}^2 E_{m^1Ag}} \tag{8}$$

where we used E_g for the energy of 1^1B_u state, since this state sets the optical gap. If we take the energy of the m^1A_g state as scaling roughly as E_g, then the energy denominator of eq 8 leads to $\gamma \propto E_g^{-3}$, as opposed to the inverse sixth power dependence of eq 1. The remaining dependence on E_g must then come from the transition moments.

The transition moment between the ground state and the 1^1B_u state can be understood in terms of the Kuhn−Thomas sum rule. This sum rule states that the sum of the oscillator strengths for optical absorption is equal to a constant. Because the 1^1B_u state carries most of the optical intensity, this implies that the oscillator strength to this state

$$f_{1^1B_u} = |\langle GS|\hat{x}|1^1B_u\rangle|^2 E_g \tag{9}$$

is a constant. For eq 9 to be constant, the transition moment must be inversely proportional to the square root of the optical gap, $|\langle GS|\hat{x}|1^1B_u\rangle| \propto E_g^{-1/2}$. Figure 6 shows a log−log plot of this transition moment versus optical gap for the PPP calculations of Figure 5. The results follow a line of slope −1/2, consistent with the predicted behavior. For eq 8 to yield $\gamma \propto E_g^{-6}$, the transition moment between the 1^1B_u and m^1A_g state must then be inversely proportional to the optical gap, $|\langle 1^1B_u|\hat{x}|m^1A_g\rangle| \propto E_g^{-1}$. Figure 7 shows that the PPP results approximately obey this proportionality, although the deviation is somewhat larger than that seen for the $|\langle GS|\hat{x}|1^1B_u\rangle|$ transition moment in Figure 6.

The dependence of the hyperpolarizability on $|\beta_1 + \beta_2|$ is examined in Figure 8, which plots $\log_{10}(\gamma)$ versus $log_{10}(|\beta_1 + \beta_2|)$ for S_{e-e} ranging from 0 to 1. The optical gap was held fixed at 2.0 eV by adjusting $2|\beta_1 - \beta_2|$. The Hückel results fit a line with slope 3, as expected because $\gamma \propto |\beta_1 + \beta_2|^3$ in eq 1. The PPP results also fit lines with slope 3, indicating that the functional dependence is the same as that of Hückel theory, $\gamma \propto |\beta_1 + \beta_2|^3$.

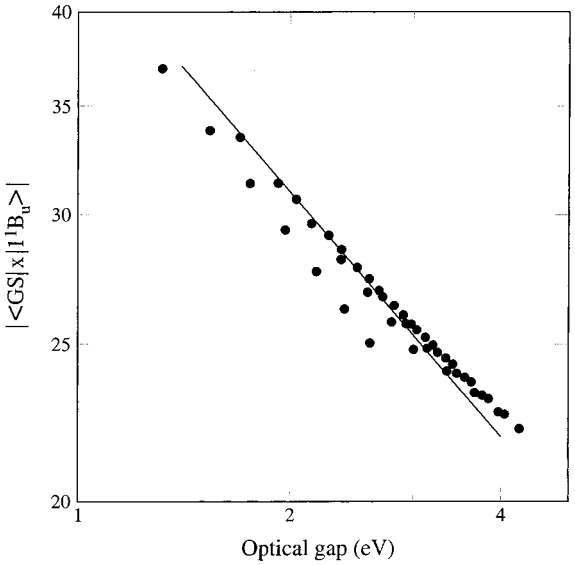

Figure 6. Log-log plot of the transition moment between the ground and 1^1B_u electronic states versus the optical gap, for the calculations of Figure 5. The line of slope $-1/2$ is provided as a guide to the eye.

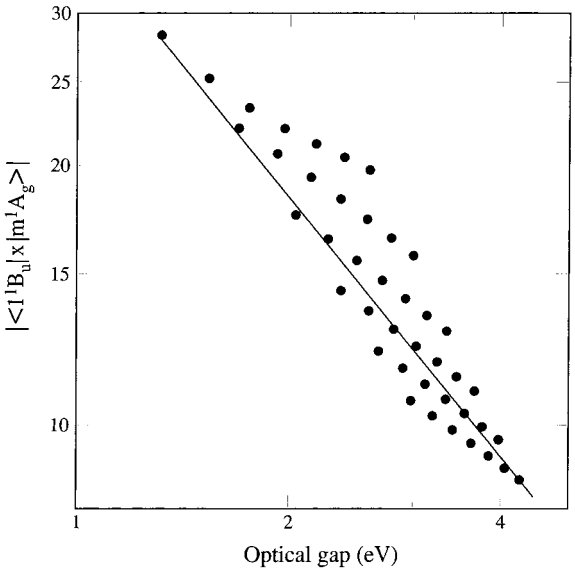

Figure 7. Log-log plot of the transition moment between the 1^1B_u and m^1A_g electronic states versus the optical gap, for the calculations of Figure 5. The line of slope −1 is provided as a guide to the eye.

The above results examine the long-chain limit of the hyperpolarizability. Figure 9 examines the dependence on chain length. Because these calculations assume periodic boundary conditions, they do not reflect the actual dependence on the length of a polyene chain. Nevertheless, they do give some indication of the relative system size needed to reach the long-chain limit. Figure 9 shows results obtained for a number of different values of $|\beta_1 - \beta_2|$, and with S_{e-e} adjusted such that the long-chain optical gap is fixed at 2.0 eV. The results show that the length at which the hyperpolarizability saturates is fairly independent of the strength of electron−electron interactions (S_{e-e}), and so depends only on the band gap and bandwidth.

B. Resonant Hyperpolarizability. The resonant hyperpolarizability associated with two-photon absorption, calculated as described in section 2.2, is shown in Figure 10. The

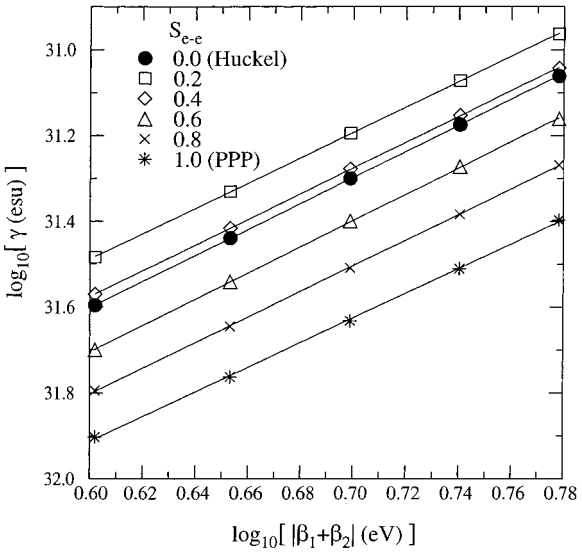

Figure 8. Log-log plot of nonresonant γ versus $|\beta_1 + \beta_2|$ from S-CI calculations on the PPP Hamiltonian for various values of S_{e-e}. $|\beta_1 - \beta_2|$ is adjusted to yield an optical gap of 2.0 eV. All other details are as in Figure 5.

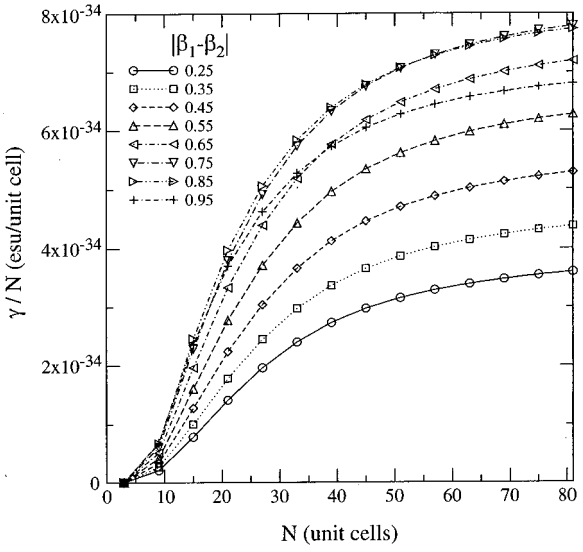

Figure 9. Plot of γ/N vs chain length (N) for $|\beta_1 - \beta_2|$ ranging from 0.25 to 0.95 eV. $(\beta_1 + \beta_2)$ is fixed at -5 eV, and S_{e-e} is adjusted such that the optical gap is 2.0 eV.

calculations were done on a polyene with 10 unit cells, using the potential of eq 7 to model the effects of ADA substitution.

The gray circles are for a polyene without an ADA potential applied. The results indicate that the resonant hyperpolarizability has a strong dependence on the optical gap. The nonresonant hyperpolarizability followed a $\gamma \propto E_g^{-6}$ dependence, and a similar dependence here would cause the points in Figure 10 to lie along a line of slope -6, such as that provided in Figure 10 as a guide to the eye. Although the results do tend toward this behavior, the spread encompasses about an order of magnitude, such that parameters that give the same optical gap can lead to resonant γ's that differ by an order of magnitude.

The black crosses are for ADA potentials of varying strength. (Due to electron−hole symmetry, DAD potentials give identical results.) The points tend toward an E_g^{-6} behavior, but with a wider spread that encompasses 2 orders of magnitude. Despite this spread, the band gap remains a predominant factor in establishing the magnitude of the response. In addition, for most sets of parameters, and all sets that lead to gaps below 3 eV,

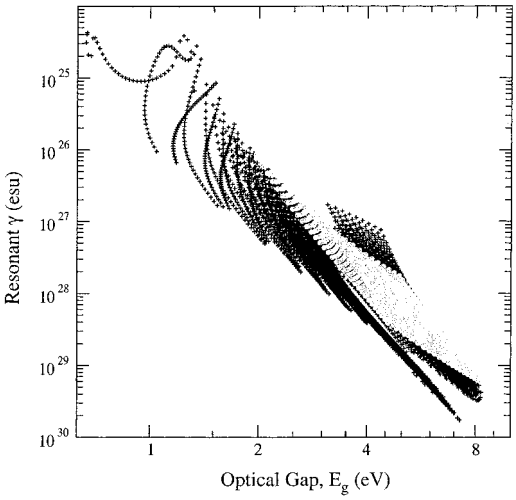

Figure 10. Log−log plot of the resonant hyperpolarizability versus the optical gap obtained from S-CI calculations on a polyacetylene chain with 10 unit cells, for both the Hückel and PPP Hamiltonians. The gray circles show γ for $|\beta_1 - \beta_2| = 0.2...2.0$ eV and $S_{e-e} = 0...2$. The black crosses show γ for the same range of PPP parameters, and with ADA acceptor−donor substitution modeled with the internal field model of eq 7 with $V = 0.1...0.5$ eV/Å.

the points for ADA substitution lie below those for the unsubstituted polyene. This indicates that for systems with equivalent optical gaps, the resonant response of the unsubstituted system will be larger than that of the ADA substituted system.

IV. Discussion

Section 1 discussed the consequences of Hückel theory for materials optimization. In Hückel theory, the nonresonant hyperpolarizability is given by eq 1, and this implies that polyacetylene is already an optimal organic material, in terms of the magnitude of the hyperpolarizability. Thus, any improvements in the figure-of-merit for optical switching applications[4] will likely come at the expense of the magnitude of the nonresonant response. This argument was, however, based on Hückel theory, a model that fails to capture many aspects of the excited electronic states that mediate the nonresonant response.[10−14]

The calculations presented here show that S-CI solutions of the PPP model of long polyene chains obey the same functional relation as Hückel theory, eq 1. Because there is strong evidence that S-CI theory provides a valid description of the nonresonant hyperpolarizability of long chains (see section 2.1), this gives strong support to the functional relation of eq 1 and its implications for materials optimization.

This observed agreement between the Hückel and PPP models is somewhat surprising, since the Coulomb interactions in the PPP Hamiltonian lead to correlated electron−hole motion and the formation of bound electron−hole pairs or excitons. The degree of electron−hole correlation may be characterized by the exciton binding energy, the energy needed to break the exciton into an unbound electron and hole. For the range of model parameters considered here, the exciton binding energy spanned from 0 to 4 eV (see Figure 3). Yet over this large range, the nonresonant hyperpolarizability is essentially independent of the exciton binding energy, instead depending almost exclusively on the band gap and bandwidth.

The dependence of the nonresonant response on the inverse-sixth power of the optical gap, $\gamma \propto E_g^{-6}$, implies that the optical transition moments depend strongly on the optical gap. Because

the energy denominator of eq 5 can account for only an inverse-third power dependence, the remainder must be in the transition moments in the numerator of eq 5. Figure 6 shows that the transition moment between the ground electronic state and the 1^1B_u state is inversely proportional to the square root of the optical gap. This is consistent with the behavior expected from the Kuhn-Thomas sum rule. In addition, Figure 7 shows that the transition moment between the 1^1B_u and m^1A_g states is inversely proportional to the optical gap. Taken together, these dependencies account for the inverse-sixth power dependence in eq 1.

Two-photon absorption is a resonant third-order nonlinear optical process and it is interesting to consider whether the optimization of this process is fundamentally different than the optimization of the nonresonant response. The results of Figure 10 show that the resonant hyperpolarizability has a strong dependence on the optical gap, scaling roughly as the inverse sixth power. However, the variance is much larger than for the nonresonant hyperpolarizability, such that two different sets of model parameters can give the same optical gap yet have resonant hyperpolarizabilities that differ by an order of magnitude. This variance becomes even larger when an internal field is used to model the effects of ADA or DAD substitution.

The symmetric charge transfer present in ADA and DAD systems has been suggested as a means to optimize the cross section for two-photon absorption. In the results of Figure 10, the hyperpolarizability of an ADA substituted polyene tends to be smaller in magnitude than that of an unsubstituted polyene with an equivalent optical gap. This does not argue against the use of such substitution patterns because they provide a useful synthetic handle while the other parameters varied in Figure 10 (the bond alternation and effective strength of electron−electron interactions) are not as easily controlled. However, these results do suggest that the ADA substitution pattern may serve primarily as a means to control the optical gap. This interpretation is somewhat different than that of Albota et al.,[27] who suggest that the symmetric charge transfer in the excited states of ADA and DAD systems increases the transition moments thereby enhancing the cross sections for two-photon absorption. However, a significant portion of the increase in transition moments can perhaps be attributed to the above dependence of the transition moments on optical gap.

The model used here to study the resonant hyperpolarizability has two potential shortcomings. First, the use of an internal field model may not accurately describe the ADA and DAD substitution patterns. Second, although S-CI theory may be adequate for studying the nonresonant response of long chains, double electron−hole pair configurations can be important for smaller systems such as the dye molecules used for two-photon absorption. Section 2.1 argues that the large positive hyperpolarizability of long chains arises from the intra-band contribution and this contribution is well described by S-CI theory. For smaller systems, the inter-band or saturable absorbance contribution can become important. Indeed, the saturable absorbance contribution dominates the response of dye molecules with low bond alternation,[36] causing these cyanine-like molecules to exhibit negative hyperpolarizability. In addition, although the nonresonant response may be insensitive to the detailed structure of individual excited states, this is not true of the resonant response. If double electron−hole pair configurations play an important role in the state that is in resonance, then S-CI theory is unlikely to provide an adequate description. Nevertheless, an examination of the experimental results of Albota et al.[27] reveals a trend with optical gap that is consistent with the scaling

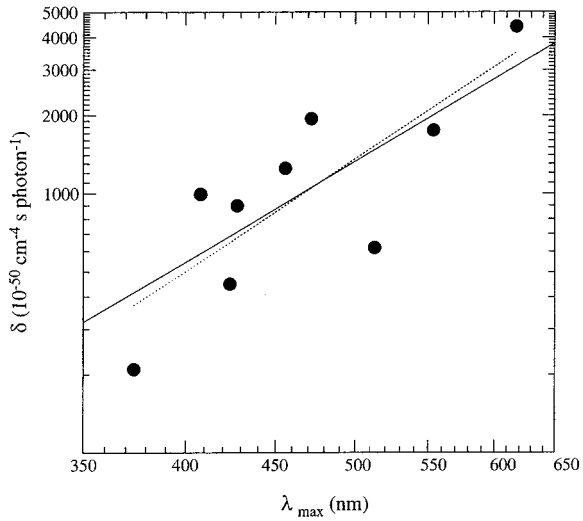

Figure 11. log−log plot of the two-photon absorption cross section versus λ_{max} for the experimental measurements of Albota et al.[27] The dotted line is the result of a linear fit, and the solid line is for $\delta \propto \lambda_{max}^4$.

obtained from S-CI theory. Figure 11 shows a log−log plot of the two-photon absorption cross section, δ, versus λ_{max}. Because $\delta \propto \omega^2\gamma$, if gamma scales as the band gap to the -6^{th} power, then δ will scale as the -4^{th} power of band gap, or the 4^{th} power of λ_{max}. Figure 11 shows that the experimental data do follow such a dependence, although there is considerable variance.

V. Conclusion

This work examines the positive, intra-band contribution to the hyperpolarizabilty that dominates the nonresonant response of long polyene chains. The results show that the response is insensitive to the strength of Coulomb interactions, and exhibits a dependence on bandwidth and optical gap that agrees with that of Hückel theory in eq 1. As discussed in the Introduction, this functional dependence on bandwidth and optical gap implies that polyacetylene is already an optimal organic material with regards to the magnitude of the hyperpolarizability.

For the resonant hyperpolarizability, the functional dependence of eq 1 holds only in terms of general trends. In the simple model of D−A−D symmetric charge transfer systems considered here, the intra-band contribution to the hyperpolarizability is roughly proportional to E_g^{-6}, but can deviate from this dependence by up to an order of magnitude. Substantial deviations from a simple scaling behavior are also seen in the experimental results of Figure 11, which show a general trend consistent with $\gamma \propto E_g^{-6}$, but with sufficient variability to allow for materials optimization by means other than controlling the optical gap. Nevertheless, in comparing various molecular engineering approaches, it is useful to take the general scaling with bandwidth and optical gap into account, noting especially that the scaling of the hyperpolarizability with optical gap arises not only from the energy denominator in the sum-over-states expression of eq 5, but also from the scaling of the transition moments with optical gap (Figures 6 and7).

Acknowledgment. This work was funded by the National Science Foundation CHE9985719.

References and Notes

(1) Chemla, D.; Zyss, J. Eds., *Nonlinear Optical Properties of Organic Molecules and Crystals*; Academic Press: New York, 1987.

(2) Bredas, J. L.; Adant, C.; Tackx, P.; Persoons, A.; Pierce, B. M. *Chem. Rev.* **1994**, *94*, 243.
(3) Fann, W.-S.; Benson, S.; Madey, J. M. J.; Etemad, S.; Baker, G. L.; Kajzar, F. *Phys. Rev. Lett.* **1989**, *62*, 1492.
(4) Stegeman, G. I.; Torruellas, W. *Mater. Res. Soc. Symp. Proc.* **1994**, *328*, 397.
(5) Denk, W.; Strickler, J.; Webb, W. *Science* **1990**, *248*, 73.
(6) Denk, W.; Svoboda, K. *Neuron* **1997**, *18*, 351.
(7) Kohler, R.; Cao, J.; Zipfel, W.; Webb, W.; Hansen, M. *Science* **1997**, *276*, 2039.
(8) Cojan, C.; Agrawal, G. P.; Flytzanis, C. *Phys. Rev. B* **1977**, *15*, 909.
(9) Agrawal, G. P.; Cojan, C.; Flytzanis, C. *Phys. Rev. B* **1978**, *17*, 776.
(10) Soos, Z. G.; Ramasesha, S.; Galvao, D. S. *Phys. Rev. Lett.* **1993**, *71*, 1609.
(11) Ohmine, I.; Karplus, M.; Schulten, K. *J. Chem. Phys.* **1978**, *68*, 2298.
(12) Mazumdar, S.; Guo, F. *J. Chem. Phys.* **1994**, *100*, 1665.
(13) Dixit, S. N.; Guo, D.; Mazumdar, S. *Phys. Rev. B* **1991**, *43*, 6781.
(14) Guo, F.; Guo, D.; Mazumdar, S. *Phys. Rev. B* **1994**, *49*, 10102.
(15) Soos, Z. G.; McWilliams, P. C. M.; Hayden, G. W. *Int. J. Quantum Chem. 1992*, *43*, 37.
(16) Soos, Z.; Etemad, E.; Kepler, R. *Mater. Res. Soc. Symp. Proc.* **1992**, *247*, 79.
(17) Mukamel, S.; Takahashi, A.; Wang, H. X.; Chen, G. *Science* **1994**, *266*, 250.
(18) Mukamel, S.; Wang, H. X. *Phys. Rev. Lett.* **1992**, *69*, 65.
(19) Halvorson, C.; Hagler, T. W.; Moses, D.; Cao, Y.; Heeger, A. J. *Chem. Phys. Lett.* **1992**, *200*, 364.
(20) Yu, J.; Friedman, B.; Baldwin, P. R.; Su, W. P. *Phys. Rev. B* **1989**, *39*, 12 814.
(21) Shuai, Z.; Bredas, J. L. *Phys. Rev. B* **1991**, *44*, 5962.
(22) Wu, C.-Q.; Sun, X. *Phys. Rev. B* **1990**, *42*, 9736.
(23) Yaron, D.; Silbey, R. *Phys. Rev. B: Condens. Matter* **1992**, *45*, 11 655.
(24) Yaron, D. *Phys. Rev. B: Condens. Matter* **1996**, *54*, 4609.
(25) Tavan, P.; Schulten, K. *Phys. Rev. B* **1987**, *36*, 4337.
(26) Kogej, T.; Beljonne, D.; Meyers, F.; Perry, J. W.; Marder, S. R.; Bredas, J. L. *Chem. Phys. Lett.* **1998**, *298*, 1.
(27) Albota, M.; Beljonne, D.; Bredas, J.-L.; Ehrlich, J. E.; Fu, J.-Y.; Heikal, A. A.; Hess, S. E.; Kogej, T.; Levin, M. D.; Marder, S. R.; et al. *Science* Washington, D. C. **1998**, *281*, 1653.
(28) Rumi, M.; Ehrlich, J. E.; Heikal, A. A.; Perry, J. W.; Barlow, S.; Hu, Z.; McCord-Maughon, D.; Parker, T. C.; Roeckel, H.; Thayumanavan, S. et al. *J. Am. Chem. Soc.* **2000**, *122*, 9500.
(29) Ohno, K. *Theor. Chim. Acta* **1964**, *2*, 219.
(30) Hinze, J.; Jaffe, H. H. *J. Am. Chem. Soc.* **1962**, *84*, 540.
(31) Spano, F. C.; Soos, Z. G. *J. Chem. Phys.* **1993**, *99*, 9265.
(32) Hasegawa, T.; Iwasa, Y.; Sunamura, H.; Koda, T.; Tokura, Y.; Tachibana, H.; Matsumoto, M.; Abe, S. *Phys. Rev. Lett.* **1992**, *69*, 668.
(33) Abe, S.; Schrieber, M.; Su, W. P.; Yu, J. *J. Lumines.* **1992**, *53*, 519.
(34) Shimoi, Y.; Abe, S. *Phys. Rev. B* **1994**, *49*, 14 113.
(35) Mukamel, S. *Principles of Nonlinear Optical Spectroscopy* (Oxford University Press: Oxford, 1995), (The THG calculations use eq 6.37. The second summation is excluded, since the solute is treated with S-CI theory.[23,24]).
(36) Marder, S. R.; Gorman, C. B.; Meyers, F.; Perry, J. W.; Bourhill, G.; Bredas, J.-L.; Pierce, B. M. *Science* **1994**, *265*, 632.
(37) In the limit of a long chain with N unit cells, there are N^2 ways to create two noninteracting excitations in γ_+, and this causes γ_+ to scale as N^2 in the long-chain limit. This N^2 dependence is canceled by a similar dependence in γ_-, such that the resulting $\gamma_+ - \gamma_-$ scales correctly as N. Since S-CI theory does not allow for the creation of two excitations, γ_+ of S-CI theory does not scale as N^2, and therefore, γ_- is not included in the evaluation of the hyperpolarizability.[23,24]